32nd International Conference
ENGINEERING MECHANICS 2026
Medlov, Czech Republic, May 11 – 13, 2026

VELOCITY CALIBRATION OF A WIND TUNNEL WITH BYPASS FLOW FOR BLADE CASCADE AEROELASTIC STUDIES

Šnábl P.[1], **Procházka P.**[2], **Skála V.**[3],

Abstract: *This paper presents a calibration methodology for an Eiffel-type wind tunnel equipped with a bypass flow system designed for aeroelastic investigations of a blade cascade subjected to a radial flow component. Since flutter onset is highly sensitive to incoming flow conditions, precise and repeatable setting of flow velocities in both the main and bypass tunnels is essential. The main tunnel velocity is determined from static pressure differences across the contraction section using Bernoulli's equation. The bypass tunnel velocity, which cannot be measured directly due to spatial and geometric constraints, is evaluated using particle image velocimetry near the blowing orifice. Velocities are measured across 30 combinations of variable-frequency drive settings of both tunnel fans. A third-order polynomial surface is fitted to the measured data using a least-square minimisation with outlier rejection. To avoid the need for numerical inversion of the fitted surfaces, dense lookup tables with linear interpolation are constructed, and iso-velocity contour diagrams are produced. The resulting calibration tool allows straightforward and reliable identification of fan frequency combinations corresponding to any desired pair of main and bypass tunnel velocities.*

Keywords: Wind tunnel calibration, Bypass flow, Particle image velocimetry, Surface fitting

1. Introduction

Modern thermal power plants are increasingly required to operate under off-design conditions due to the growing share of intermittent renewable energy sources in the power grid. Under such conditions, reduced mass flow alters the pressure distribution within the turbine stages, strengthening the radial velocity component and modifying the effective angle of attack of the blades. This promotes flow separation and increases the risk of aeroelastic instabilities, particularly stall flutter, which can lead to severe blade damage. The last stage of the low-pressure turbine is especially susceptible due to its long, slender blades and low-camber profiles Procházka et al. (2026).

To study such phenomena experimentally, an Eiffel-type wind tunnel with a 700 mm × 700 mm square cross-section, driven by a 14 kW axial fan, has been equipped with a bypass flow system. The bypass tunnel introduces a controlled cross-flow jet into the main test section through a blowing orifice located upstream of the blade roots, while a suction orifice downstream of the blade tips closes the bypass loop. The bypass duct, driven by an independent radial fan, has a cross-sectional area approximately eight times smaller than that of the main tunnel, so that comparable jet and main-flow velocities can be achieved at a proportionally lower bypass flow rate. A fine mesh screen at the blowing orifice homogenises flow non-uniformities originating from the elbow wakes in the bypass piping. The initial design idea is described in Šnábl et al. (2024) and the experimental facility CAD model is shown in Fig. 1.

Because flutter onset is highly sensitive to incoming flow conditions, precise and repeatable setting of the operating point is essential for the planned aeroelastic investigations. Unlike the main tunnel, the bypass duct contains neither a contraction nor a sufficiently long straight pipe section to allow reliable direct flow-rate measurement. As demonstrated in Procházka et al. (2026), where the bypass jet topology was characterised using particle image velocimetry (PIV), the interaction between the bypass jet and the main

[1] Ing. Pavel Šnábl: Ústav termomechaniky AV ČR, v. v. i., Dolejškova 1402/5; 182 00, Prague; CZ, snabl@it.cas.cz
[2] Ing. Pavel Procházka, PhD.: Ústav termomechaniky AV ČR, v. v. i., Dolejškova 1402/5; 182 00, Prague; CZ, prochap@it.cas.cz
[3] Ing. Vladislav Skála, PhD.: Ústav termomechaniky AV ČR, v. v. i., Dolejškova 1402/5; 182 00, Prague; CZ, skala@it.cas.cz

ISSN: 1805-8256, doi: 10.21495/em2026-129

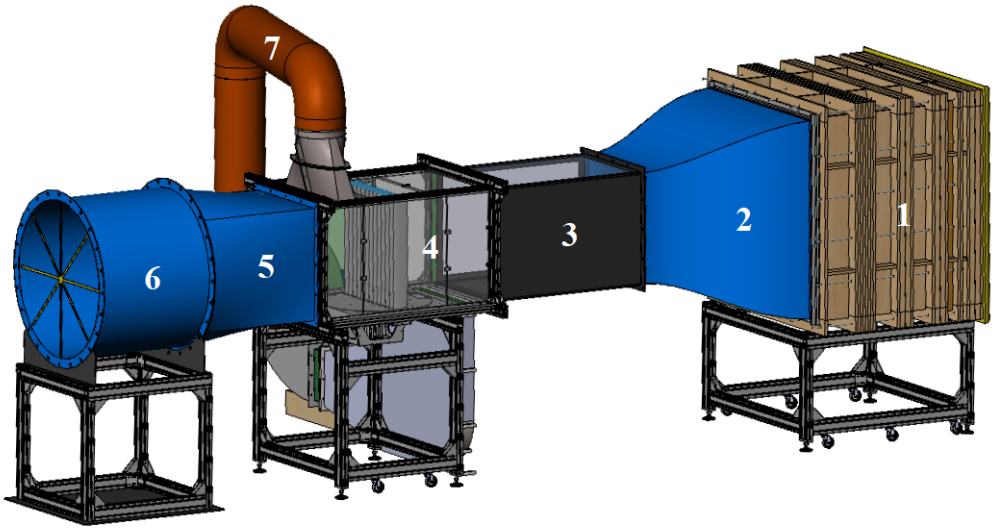

Fig. 1: CAD model of the wind tunnel with bypass flow: 1 – settling chamber, 2 – contraction, 3 – test section extension, 4 – test section, 5 – diffuser, 6 – main tunnel fan, 7 – bypass loop.

tunnel flow is complex: the jet deflects and narrows with increasing main tunnel velocity, and the penetrating jet imposes an additional pressure loss on the main tunnel, requiring simultaneous adjustment of both fan speeds. This coupling motivates the need for a systematic calibration of the two-tunnel system. The present paper therefore focuses on the velocity evaluation methodology, surface fitting of the measured data, and the construction of a practical iso-velocity diagram that allows straightforward identification of the fan frequency settings corresponding to any desired pair of main and bypass tunnel velocities.

2. Evaluation of Velocities

2.1. Main Tunnel

The main tunnel velocity was calculated from measured pressure difference on the contraction (2 in Fig. 1). From the Bernoulli's equation for incompressible flow we have:

$$p_A + \frac{1}{2}\rho v_A^2 = p_B + \frac{1}{2}\rho v_B^2 + p_L, \tag{1}$$

where p_A and p_B are pressures at the contraction inlet and outlet, v_A and v_B are velocities at the contraction inlet and outlet and ρ is the air density. The pressure loss p_L is neglected, as it is expected to be lower than the resolution of our pressure sensor.

From the continuity equation for the incompressible flow we get:

$$A v_A = B v_B, \tag{2}$$

where A and B are the respective inlet and outlet areas of the contraction. By substituting of v_B from (2) into (1) and rearranging, we get an equation to calculate the contraction outlet velocity, i.e. the main tunnel velocity, from pressure difference on the contraction inlet and outlet:

$$v_B = \sqrt{\frac{2(p_A - p_B)}{\rho\left[1 - \left(\frac{B}{A}\right)^2\right]}}. \tag{3}$$

2.2. Bypass Tunnel

The bypass velocity was measured by using particle image velocimetry in a plane located in the middle of the tunnel width above the bypass inlet. The velocities were evaluated at horizontal line 20 mm above the tunnel floor. Further information about the evaluation procedure is described in Procházka et al. (2026).

3. Velocities Surface Fitting

Variable-frequency drives (VFD) of the main and bypass tunnel motors were set in all combinations of the following frequencies: $f_M = (10,\ 20,\ 30,\ 40,\ 50)\,\mathrm{Hz}$ and $f_B = (0,\ 10,\ 20,\ 30,\ 40,\ 50)\,\mathrm{Hz}$. Measurements were not performed for $f_M = 0\,\mathrm{Hz}$ since the bypass flow is intended only for modification of the main tunnel flow. Turning on the bypass only actually creates a backflow in the main tunnel.

Several other measurements had to be discarded from the measured data sets:

- Main tunnel velocity measurement at $f_M = 10\,\mathrm{Hz}$ and $f_B = (30,\ 40,\ 50)\,\mathrm{Hz}$ — at those VFD frequencies the bypass flow dominates, hits the top wall of the tunnel and creates big recirculation area in the test section extension (3 in Fig. 1) and possibly disturbs the pressure measurement on the contraction.
- Bypass tunnel measurement at $f_M = (30,\ 40,\ 50)\,\mathrm{Hz}$ and $f_B = 10\,\mathrm{Hz}$ — here, the bypass outlet velocity is negligible to the main tunnel velocity and the particle-saturated bypass air is blown away before reaching the evaluation line for the PIV measurement.
- Bypass tunnel measurement at $f_M = (0,\ 10)\,\mathrm{Hz}$ and $f_B = 50\,\mathrm{Hz}$ — not enough particles were fed into the bypass tunnel and the PIV evaluation was unreliable.

All of the kept measured velocities are plotted in Fig. 2 as circles.

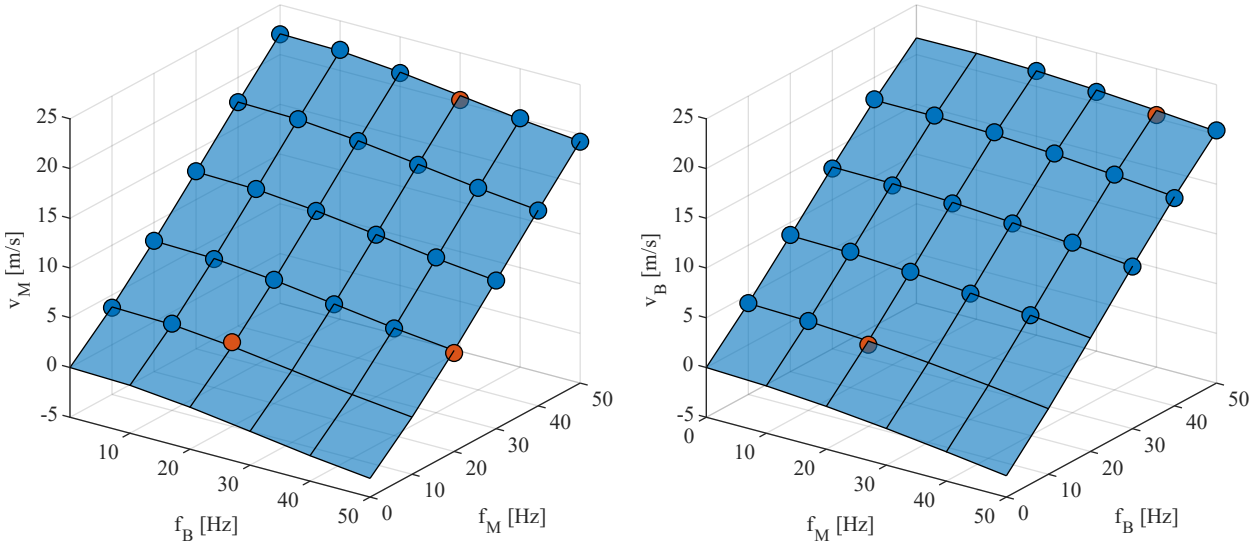

(a) Main tunnel velocity. *(b) Bypass tunnel velocity.*

Fig. 2: Measured main tunnel velocities v_M and bypass tunnel velocities v_B for main and bypass tunnel frequencies f_M and f_B with fitted surfaces.

Next, surface fitting was performed to obtain functions for main and bypass tunnel velocities. As a suitable function, a 7-parameter third order polynomial surface was chosen for both velocities:

$$v = c_1 f_M + c_2 f_M^2 + c_3 f_M^3 + c_4 f_B + c_5 f_B^2 + c_6 f_B^3 + c_7 f_M f_B. \tag{4}$$

To obtain well-fitting function, a 3-step fitting was performed using a least-square error minimisation:

1. The function constants were fitted using all of the measured data points.
2. Points with residuals higher than $1.5\times$ the standard deviation were discarded as outliers (red points in Fig. 2).
3. The function constants were re-fitted after discarding the outliers.

The fitted surface functions for both main tunnel and bypass tunnel velocities are shown in Fig. 2.

At the end, an inverse task had to be solved. For given flow velocities, we need the corresponding VFD frequencies. Since the velocity functions given by (4) are not linear, the inverse functions would need to be solved numerically. To overcome the numerical solution, that could experience numerical instability, find multiple solutions etc., a more practical engineering approach was chosen. Velocities were calculated for frequencies with small increment, creating dense lookup tables. Linear interpolation was then used to find

the frequencies corresponding to the chosen velocity pair. Also, the data from the lookup tables were used to construct the graph in Fig. 3 with velocity isolines over the frequencies grid that allows to find the desired operating point optically.

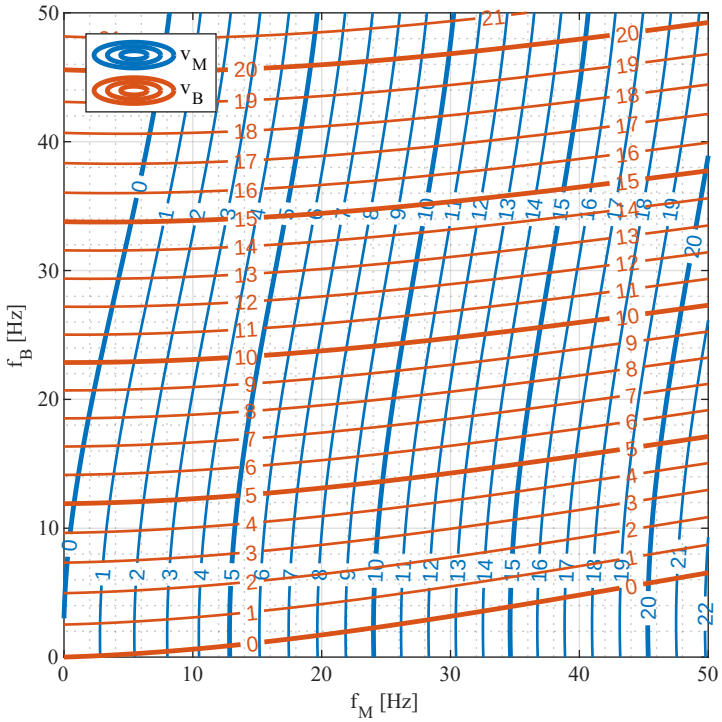

Fig. 3: Isolines of main tunnel velocity v_M and bypass tunnel velocity v_B for main and bypass tunnel frequencies f_M and f_B.

4. Conclusions

A calibration methodology for a coupled main and bypass wind tunnel system has been developed and validated. Main tunnel velocities were determined from contraction pressure differences, while bypass velocities were evaluated using PIV. A third-order polynomial surface fitted to the measured data, combined with outlier rejection, provided accurate velocity predictions across the full operating range. The resulting lookup tables and iso-velocity diagram enable straightforward and repeatable setting of desired flow conditions, providing a reliable basis for future aeroelastic investigations of the blade cascade under controlled radial flow.

Acknowledgments

This work was supported by the project GA26-22907S: “Friction-induced instabilities in dynamic systems with rolling-sliding contact under transient conditions”

References

Procházka, P., Šnábl, P., and Skála, V. (2026) On the calibration of the bypass tunnel used for cascade aeroelastic study. In Zolotarev, I., Pešek, L., and Kozień, M., eds, *DYMAMESI 2026 Proceedings*, Prague. Institute of Thermomechanics of the CAS, Prague, pp. 43–46.

Šnábl, P., Pešek, L., Procházka, P., and Prasad, C. S. (2024) Computer-aided engineering in the design of an experimental blade cascade for fluid-structure interaction studies. In Beran, J., Bílek, M., Václavík, M., and Žabka, P., eds, *Advances in Mechanism Design IV: Proceedings of TMM 2024*, Cham. Springer, pp. 114–122.